

range determined in part by the pressure of their normal environment (7) and by their position in the taxonomic hierarchy (11, 12). Thus, the bacterium CNPT-3 from an environment of 580 bars survived and grew at atmospheric pressure. Yet, a bacterium, isolate MT-41, from an environment of 1062 bars died at atmospheric pressure. A group of greater biological complexity, the amphipods (arthropods), from the same depth as bacterial strain CNPT-3, died at atmospheric pressure (12).

Pressures exceeding the maximum pressure permitting growth kills organisms. This has been shown for various prokaryotic cells (2). Our study shows that pressures lower than those permitting growth can also kill avacuolate microorganisms.

Sensitivity to decompression can arise from the presence of organs or organelles containing gases (13) and from the temporal aspects of pressure changes. Such factors acting in concert can lead to complex mechanisms of death due to decompression. Only in bacteria containing gas vesicles that expand on decompression, causing the cell wall and membrane to burst, is the mechanism of cell death clear (13). Methods (14, 15) that permit colonies to grow in the complete absence of decompression may allow for the discovery of gas-vacuolated bacteria in the deep sea.

A. ARISTIDES YAYANOS
ALLAN S. DIETZ

*Physiological Research Laboratory,
Scripps Institution of Oceanography,
University of California, San Diego,
La Jolla 92093*

References and Notes

1. J. W. Deming, P. S. Tabor, R. R. Colwell, *Microb. Ecol.* **7**, 85 (1981).
2. R. E. Marquis and P. Matsumura, in *Microbial Life in Extreme Environments*, D. J. Kushner, Ed. (Academic Press, London, 1978), pp. 135-138.
3. A. A. Yayanos and A. S. Dietz, *Appl. Environ. Microbiol.* **43**, 1481 (1982).
4. ———, R. Van Boxtel, *Science* **205**, 808 (1979).
5. ———, *Proc. Natl. Acad. Sci. U.S.A.* **78**, 5212 (1981).
6. A. A. Yayanos, R. Van Boxtel, A. S. Dietz, K. M. Jones, *Abstracts, 80th Annual Meeting (American Society for Microbiology, Washington, D.C., 1980)*, p. 173.
7. A. A. Yayanos, A. S. Dietz, R. Van Boxtel, *Appl. Environ. Microbiol.* **44**, 1356 (1982).
8. C. E. ZoBell, *Science* **115**, 507 (1952).
9. ——— and R. Y. Morita, *J. Bacteriol.* **73**, 563 (1957).
10. ———, *Galathea Rep. Copenhagen* **1**, 139 (1959).
11. A. G. Macdonald and I. Gilchrist, *Comp. Biochem. Physiol. A* **71**, 349 (1982).
12. A. A. Yayanos, *ibid.* **69**, 563 (1981).
13. B. B. Hemmingsen and E. A. Hemmingsen, *J. Bacteriol.* **143**, 841 (1980).
14. H. W. Jannasch, C. O. Wirsen, C. D. Taylor, *Science* **216**, 1315 (1982).
15. A. S. Dietz and A. A. Yayanos, *Appl. Environ. Microbiol.* **36**, 966 (1979).
16. Supported by a contract from Sandia National Laboratories and by grant OCE79-08972 from the National Science Foundation.

1 July 1982; revised 9 December 1982

Electron Microscope Tomography: Transcription in Three Dimensions

Abstract. *Three-dimensional reconstruction of an asymmetric biological ultra-structure has been achieved by tomographic analysis of electron micrographs of sections tilted on a goniometer specimen stage. Aligned micrographs could be displayed as red-green three-dimensional movies. The techniques have been applied to portions of in situ transcription units of a Balbiani ring in the polytene chromosomes of the midge Chironomus tentans. Current data suggest a DNA compaction of about 8 to 1 in a transcription unit. Nascent ribonucleoprotein granules display an imperfect sixfold helical arrangement around the chromatin axis.*

The objective of the tomographic method is the formation of an image of the internal structure of an object from a series of projections. Computerized axial tomography, made possible by advances in applied mathematics and computer technology (1), is well known in medical imaging and other fields. Application to electron microscopy has heretofore been limited to objects with known symmetry, such as crystalline materials (2) or those with a well-defined cylindrical form (3). In this report, we describe electron microscope tomography (EMT) of objects lacking any apparent internal symmetry or predetermined orientation and thus applicable to many cellular structures in situ.

A series of electron micrographs of a specimen tilted around a single arbitrary axis is prepared. The micrographs constitute a set of magnified projections viewed at various tilt angles. The projections are combined, via their Fourier transforms in the direction perpendicular to the tilt axis, to yield the three-dimensional image. Ideally, projections spanning 180° of tilt should be used; in practice, the specimen shape and the mechanical limitations of tilt stages and specimen grids preclude tilts beyond ±60°. The image constructed from incomplete data exhibits decreased resolution in the direction of the missing views (4); nonetheless, sufficiently detailed and informative reconstructed images are obtained to warrant further use of the technique.

The sequence of operations as applied to sectioned specimens can be outlined as follows. Sections up to 0.25 μm thick were mounted on clean copper grids with the support film omitted in order to achieve complete stain penetration. Carbon coating followed the staining procedure. A colloidal suspension of gold was applied to both surfaces of the stained plastic section. These spherical gold particles constitute the reference points for relating the different tilt views. Areas for tomographic reconstruction were chosen by studying stereo pairs. A tilt series was then obtained on a microscope equipped

with a eucentric goniometer (consequently, the objective lens current did not change throughout the series). Micrographs were taken at intervals of 5° to 10° between ±60°.

In an earlier reconstruction from electron micrographs of paramyosin filaments (3), the rod-shaped objects had been carefully aligned in the microscope to be parallel to the tilt axis. The spatial correlation of the micrographs along the tilt axis was accomplished by visual registration of images of the cylindrical structure and gold particles. In the present case, the arbitrary orientation of the object necessitated a more elaborate procedure. Digitization of the micrographs preceded the alignment step; a Vidicon scanning camera was mounted above a light box equipped with a micrometer-controlled stage, and connected to an image-processing system (International Imaging Systems model 70). The rasterized image is 512 × 512 pixels, with resolution controlled by the distance from the negative to the camera. (In the present study 1 pixel was set equal to about 3 nm of specimen structure.) The Vidicon camera has the virtue of a high refresh rate (30 sec⁻¹), which facilitates interactive positioning of the negative.

For each micrograph, alignment and registration require the determination of the rotation angle which orients the micrograph with the projection of the tilt axis in a standard direction; in addition, two independent translations are required in order to achieve a common origin of coordinates. Our program (5) establishes best values of these parameters by a least-squares fit between the observed positions of the gold spheres, estimated from the digitized images of all micrographs in a tilt series, and their calculated positions. Additional useful parameters evaluated by the least-squares program include best values of the tilt angles (precise to within 0.1°), magnification ratios between tilted and untilted projections, and Cartesian coordinates of the gold spheres. When the translations and rotation angles are established, each micrograph is again digi-

tized in the proper position and orientation by adjusting the translation-rotation stage to cause the new "live" image to be superimposed exactly on a rotated and translated display of its predecessor; this procedure avoids the resolution loss from the interpolation required in the computer rotation of a digitized image. In addition to the tomographic reconstruction, this program has permitted the generation of red-green stereo movies of the tilting biological structure by fanning through successive image memory planes.

After each pixel intensity value has been converted to the logarithm of absorbance, a one-dimensional fast Fourier-transform algorithm is applied to each row. Transforms of corresponding rows from all the tilt images are combined to build up two-dimensional transforms in planes perpendicular to the tilt axis. Fourier space between the central sections is filled through bilinear interpolation (3), with a linear attenuation of values extrapolated from the $\pm 60^\circ$ projections into the sectors devoid of data, and a radial decay factor is applied to reduce series termination errors. Stain density patterns are clearly visible in the back transforms. Several artifacts also appear and are attributable in part to the problem of incomplete data (4) and in part to "contamination" of the projections at the higher tilt angles with extraneous density due to structures in the specimen outside the reconstructed volume. When examined on a sophisticated image-processing system, the displayed images can be enhanced to minimize artifacts and emphasize regions with significant density. The three-dimensional matrix of calculated densities can be "sliced," bounded projections can be computed, and the result may be viewed from any desired direction.

The factors limiting resolution (2, 4) in the reconstructed image include finite pixel density, finite increments in tilt angle, the extent of the wedge of unobserved projections, and the radial decay function. We estimate that in the reconstructions presented here the resolution ranges from 5 to 7.5 nm, with the larger value corresponding to the thickness dimension of the specimen. Better resolution through use of greater magnification, higher pixel density, and more tilt views is clearly possible.

The polytene chromosomes of the salivary gland of fourth-instar larvae of *Chironomus tentans* display one of the clearest microscopically observable examples of gene transcription, the Balbiani rings. Approximately 10^4 identical endoreplicated chromatid strands asso-

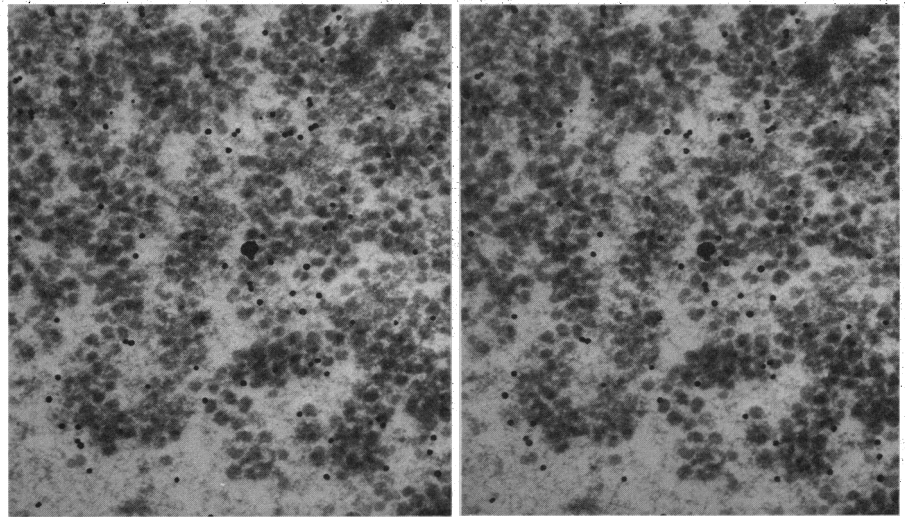


Fig. 1. A longitudinal section of a loop containing most of a Balbiani ring transcription unit. In this pair of stereo electron micrographs, the more mature transcripts, packaged into 45- to 50-nm RNP granules and attached to the presumptive chromatin axis by stems, are seen at the left side of the loop. The right side of the loop contains the less mature transcripts, which look like the stems without the characteristic Balbiani ring granule. This ring is from a fourth-instar larva exposed to pilocarpine for 5½ hours (7, 8). Under these conditions, BR2 produces approximately ten times as much 37-kilobase messenger RNA as is found in untreated animals, without an apparent increase in granule density per micrometer of chromatin axis in situ (8). The tilt axis is vertical. Tilt angles are $\pm 6^\circ$ and the magnification is $\times 39,000$.

ciate to form the characteristic polytene chromosomes with bands and interbands. The short fourth chromosome normally displays two very large puffs, Balbiani rings BR2 and BR1. Biochemical and cytological evidence (6) has established that these puffs are the sites of synthesis of a 37-kilobase messenger RNA that codes for a very high molecular weight (approximately 10^6 daltons) secretory protein.

The active genes of the Balbiani rings have a distinctive ultrastructure that facilitates their examination in situ (Fig. 1). Transcription axes can be readily observed in sections through the genes, and portions of hundreds of transcription units can be found in a single section. Regions of mature ribonucleoprotein (RNP) exhibit characteristic electron-dense Balbiani ring granules 45 to 50 nm in diameter that are connected by short stems to the chromatin axes (8, 9). The morphology of active Balbiani ring genes has also been examined by spreading swollen isolated fourth chromosomes (10). Under these conditions the transcription units of the genes are about 7.7 μm long (indicating DNA compaction by a factor of 1.6), and each transcription unit contains approximately 125 RNP with an average density of 16 RNP per micrometer of spread chromatin axis. Furthermore, tandem repeats of the genes along a single chromatid strand were never observed. Since that study, we (8) and Danholt (9) have attempted to measure the quantity of RNP per

micrometer of chromatin axis and to calculate the DNA compaction factor in situ. Both groups independently arrived at similar values (30 to 40 RNP per micrometer, corresponding to a DNA compaction factor of 3 to 4). During the past year it has become clear to us that this estimate of transcript density is too low. Examining thicker sections (200 to 250 nm instead of 100 nm) has resulted in higher density estimates. Since mature regions of transcription units have an outer diameter of approximately 200 nm, sections 100 nm thick cannot contain the entire width of the Balbiani ring transcription axes. The density and arrangement of Balbiani ring RNP in a transcription axis can be profitably studied by application of EMT to sufficiently thick sections.

Spatially correlated tilt images of the Balbiani ring transcription axes were examined on the image-processor display by fanning back and forth through adjacent angles to generate red-green stereo "movies." Generally, two categories of views, longitudinal and cross-sectional, were chosen for further study.

An illustrative set of calculated slices through a cross section of a transcription unit are presented in Fig. 2. The various sections were contoured, traced, cut out of balsa sheets, and stacked to provide an image of the transcription axis in three dimensions (Fig. 3).

On the basis of current model building, the following structural features have emerged: well-formed regions appear to

contain about 80 Balbiani ring granules per micrometer of chromatin axis, possibly in an imperfect helical pattern with a pitch of approximately 70 nm. Frequently, cross-sectional views (Fig. 2) exhibit hexagonal or heptagonal patterns. The Balbiani ring granules exhibit clear internal structure suggestive of coiling of nascent RNP. The higher estimate of RNP density implies a greater DNA compaction factor in situ than was previously calculated (8, 9). Our present estimate of a factor of about 8 is not very different from values predicted for nucleosomal DNA but is still less than the compaction factor calculated for chromatin folded

into the 20 to 30 nm higher order fibers. The estimated DNA compaction factor indicates that a single transcription unit in situ would have a length of approximately 2 μm . Thus the loop shown in Fig. 1 would constitute the major fraction of an entire transcription unit. Further studies will be needed to test and refine the structural parameters cited above, to determine the helical sense, and to extend the analysis into more immature regions of the transcribing Balbiani ring genes.

Note added in proof: After submission of this manuscript, we measured the apparent path of the central chromatin

axis as defined by the insertion points of the RNP stems. The chromatin axis appeared to be coiled, with a foreshortening of approximately 4 to 1, suggesting that the overall arrangement and density of RNP may be a composite of different levels of DNA folding.

DONALD E. OLINS

ADA L. OLINS

*University of Tennessee—Oak Ridge
Graduate School of Biomedical
Sciences and Biology Division,
Oak Ridge National Laboratory,
Oak Ridge, Tennessee 37830*

HENRI A. LEVY

*Chemistry Division,
Oak Ridge National Laboratory*

RICHARD C. DURFEE

STEPHEN M. MARGLE

ED P. TINNEL

*Computer Sciences,
Oak Ridge National Laboratory*

S. DAVID DOVER

*Department of Biophysics,
King's College, University of London,
London WC2B 5RL, England*

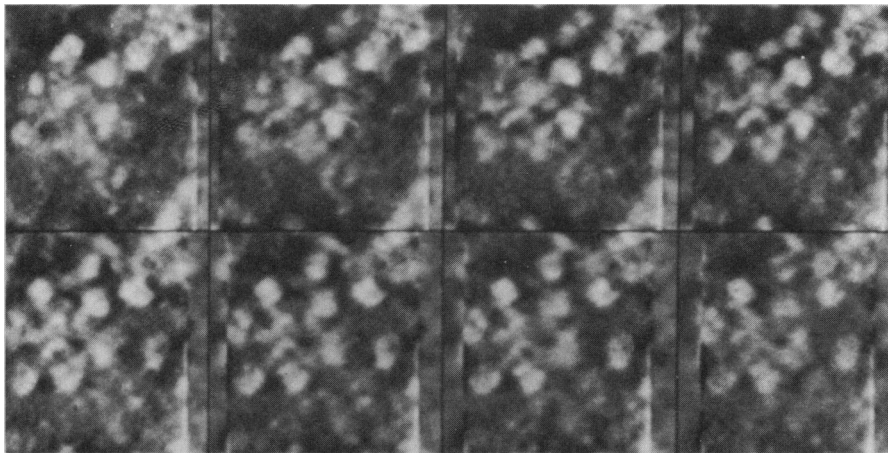


Fig. 2. Eight consecutive parallel sections from a sequence of 64 through a tomographic reconstruction (128 pixels)³ of a Balbiani ring transcription unit. The tilt axis is vertical. The series starts with the upper left frame and terminates with the lower right frame. Contrast is reversed, so that Balbiani ring granules appear light against a dark background. Each frame is 400 nm² and displays the sum of two adjacent computed sections, making each frame about 6 nm thick. This region of mature transcripts clearly shows the 45-nm Balbiani ring granules attached by stems to the presumptive central chromatin axis, with approximately sixfold rotational symmetry.

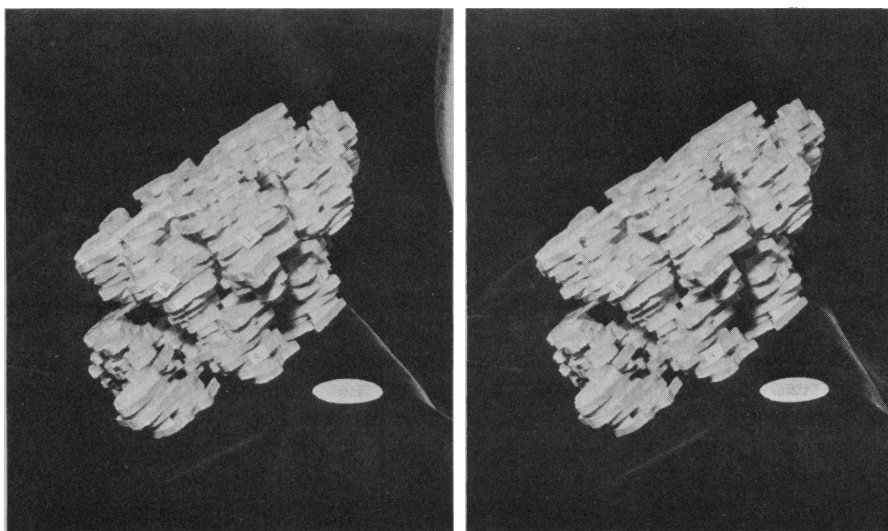


Fig. 3. Stereo photographs of a balsa wood model of a portion of a transcription unit of Balbiani ring. The axis of the transcription unit is approximately vertical in these photographs. An apparent helical arrangement of Balbiani ring granules can be readily observed. The scale marker at the lower right hand corner of the model is 45 nm wide.

References and Notes

1. G. L. Brownell, T. F. Budinger, P. C. Lauterbur, P. L. McGeer, *Science* **215**, 619 (1982); G. T. Herman, *Image Reconstruction from Projections* (Academic Press, New York, 1980).
2. R. A. Crowther, D. J. DeRosier, A. Klug, *Proc. R. Soc. London Ser. A* **317**, 319 (1970); J. E. Mellema, *Top. Curr. Phys.* **13**, 89 (1980).
3. S. D. Dover, A. Elliott, A. K. Kernaghan, *J. Microsc. (Oxford)* **122**, 23 (1981).
4. W. Hoppe and R. Hegerl, *Top. Curr. Phys.* **13**, 127 (1980).
5. H. A. Levy and S. D. Dover, manuscript in preparation.
6. W. Beermann, in *Results and Problems in Cell Differentiation*, W. Beermann, Ed. (Springer-Verlag, Berlin, 1972), vol. 4, p. 1; J. E. Edström, in *The Cell Nucleus*, H. Busch, Ed. (Academic Press, New York, 1974), vol. 2, p. 293; B. Daneholt, in *Insect Ultrastructure*, M. Akai and R. King, Eds. (Plenum, New York, 1982), in press.
7. R. Mähr, B. Meyer, B. Daneholt, H. M. Eppenberger, *Dev. Biol.* **80**, 409 (1980); M. Lezzi, B. Meyer, R. Mähr, *Chromosoma* **83**, 327 (1981); B. Meyer, R. Mähr, H. M. Eppenberger, M. Lezzi, *Dev. Biol.*, in press.
8. A. L. Olins, D. E. Olins, W. W. Franke, *Eur. J. Cell Biol.* **22**, 714 (1980); A. L. Olins, D. E. Olins, M. Lezzi, *ibid.* **27**, 161 (1982).
9. K. Andersson, B. Björkroth, B. Daneholt, *Exp. Cell Res.* **130**, 313 (1980).
10. M. M. Lamb and B. Daneholt, *Cell* **17**, 835 (1979).
11. We thank E. Wilkinson-Singley for technical assistance, M. Hsu-Hsie and J. Finch for photographic assistance, E. Uberbacher and G. J. Bunick for helpful suggestions, J. Dubochet and T. Arad of the European Molecular Biology Laboratory, Heidelberg, and J. Bentley of Oak Ridge National Laboratory for use of their Philips 400 electron microscopes, and M. Lezzi for biologic specimens. Supported by seed money from Oak Ridge National Laboratory (to D.E.O. and R.C.D.), by grant CD-113 from the American Cancer Society (to A.L.O. and D.E.O.) NIH grant GM-19334 (to D.E.O.), NIH grant GM-29429 (to A.L.O.), a grant from the Wellcome Foundation (to S.D.D.), and by Department of Energy contract W-7405-eng-26 with Union Carbide Corporation. Blocks for electron microscopy were prepared while D.E.O. was a recipient of a senior U.S. scientist award from the Alexander von Humboldt Foundation. An abstract of this work was presented at the 22nd annual meeting of the American Society for Cell Biology (*J. Cell Biol.* **95**, 66a, 1982).

20 September 1982; revised 15 December 1982